Experimental Investigation of Lee–Yang Criticality Using Non-Hermitian Quantum System

Ziheng Lan(蓝子桁)[1,2†], Wenquan Liu(刘文权)[1,2,4†], Yang Wu(伍旸)[1,2*], Xiangyu Ye(叶翔宇)[1,2], Zhesen Yang(杨哲森)[5], Chang-Kui Duan(段昌奎)[1,2,3], Ya Wang(王亚)[1,2,3], and Xing Rong(荣星)[1,2,3]

[1]*CAS Key Laboratory of Microscale Magnetic Resonance and School of Physical Sciences, University of Science and Technology of China, Hefei 230026, China*
[2]*CAS Center for Excellence in Quantum Information and Quantum Physics, University of Science and Technology of China, Hefei 230026, China*
[3]*Hefei National Laboratory, University of Science and Technology of China, Hefei 230088, China*
[4]*School of Science, Beijing University of Posts and Telecommunications, Beijing 100876, China*
[5]*Kavli Institute for Theoretical Sciences, Chinese Academy of Sciences, Beijing 100190, China*

(Received 23 November 2023; accepted manuscript online 12 April 2024)

Lee–Yang theory clearly demonstrates where the phase transition of many-body systems occurs and the asymptotic behavior near the phase transition using the partition function under complex parameters. The complex parameters make the direct investigation of Lee–Yang theory in practical systems challenging. Here we construct a non-Hermitian quantum system that can correspond to the one-dimensional Ising model with imaginary parameters through the equality of partition functions. By adjusting the non-Hermitian parameter, we successfully obtain the partition function under different imaginary magnetic fields and observe the Lee–Yang zeros. We also observe the critical behavior of free energy in vicinity of Lee–Yang zero that is consistent with theoretical prediction. Our work provides a protocol to study Lee–Yang zeros of the one-dimensional Ising model using a single-qubit non-Hermitian system.

DOI: 10.1088/0256-307X/41/5/050301

Investigating the phase transitions of many-body systems helps to understand their physical properties under different parameters. In vicinity of the phase transition, the characteristics of the system will change drastically with small changes of parameters.[1,2] Lee and Yang generalized the control parameters to the complex plane in order to characterize the phase transition with the zeros of partition function.[3,4] At the thermodynamic limit, the complex control parameters for partition function zeros approach the point on the real axis, where a phase transition occurs. The theoretical framework of Lee and Yang has been widely applied to various systems, such as folded proteins,[5,6] complex networks,[7,8] and Bose–Einstein condensation.[9,10]

Experimentally investigating Lee–Yang theory is challenging because it requires the system to be under imaginary control parameters, while physical systems are usually under real parameters. Early experiments derive the densities of Lee–Yang zeros from susceptibility measurement and analytic continuation.[11,12] One possible approach is to measure the coherence of probe spins coupled to the system to realize the observation of Lee–Yang zeros.[13] Some progresses have been made with this approach in the nuclear magnetic resonance[14] and trapped ions system.[15] However, this approach achieves the measurement of the partition function zeros by equating the evolution time in the dynamic process with the imaginary parameter. Thus, a directly constructing and studying the Lee–Yang critical behavior of a system under an imaginary parameter is still absent.

Here we build up a non-Hermitian quantum system using nitrogen-vacancy (NV) center to investigate the Lee–Yang criticality of the one-dimensional Ising model. On the basis of quantum-classical correspondence,[16,17] the classical one-dimensional Ising model at complex values of the magnetic field is mapped to a single qubit quantum system governed by the non-Hermitian Hamiltonian via the equivalent canonical partition function.[18] Thus, the corresponding quantum system features the thermodynamic properties of the classical model under complex parameters. The partition functions of the one-dimensional Ising model with different imaginary magnetic fields are experimentally obtained from the evolution under the non-Hermitian Hamiltonians, which determines the Lee–Yang zeros. Furthermore, the critical behaviors of free energy in vicinity of the Lee–Yang zero are observed from the corresponding partition function. Our work provides a route for investigating the thermodynamic properties of the classical one-dimensional Ising model under complex control parameter utilizing the non-Hermitian quantum system.

A prototypical example exhibiting the Lee–Yang criticality is the classical one-dimensional Ising model with N

†These authors contributed equally to this work.
*Corresponding author. Email: wuyanga@ustc.edu.cn
© 2024 Chinese Physical Society and IOP Publishing Ltd

particles:

$$H_{\rm Ising} = -J\sum_{j=1}^{N}\sigma_j\sigma_{j+1} - ih_{\rm cl}\sum_{j=1}^{N}\sigma_j, \tag{1}$$

where J is the ferromagnetic interaction and the operators σ_j take values ±1. As presented by Lee and Yang,[3,4] the Lee–Yang zeros of the Ising model are located on the axis where the magnetic field is imaginary. Therefore the external magnetic field is set to be a pure imaginary value $ih_{\rm cl}$ ($h_{\rm cl}\in\mathbb{R}$). Under the periodic boundary condition and the thermodynamic limit $N\to\infty$, this classical model can be mapped to a quantum system through the quantum-classical correspondence. The Ising model and its corresponding quantum system have equivalent partition function. Here we consider a non-Hermitian Hamiltonian $H_{\rm Q} = h_x\sigma_x + ih_z\sigma_z$ with real parameters h_x and h_z. The partition function for $H_{\rm Q}$ is given by

$$Z_{\rm Q} = {\rm Tr}[e^{-\beta H_{\rm Q}}] = {\rm Tr}[e^{\beta H_{\rm Q}}] = \sum_{\sigma_0=\pm1}\langle\sigma_0|e^{\beta H_{\rm Q}}|\sigma_0\rangle, \tag{2}$$

where $\beta = 1/k_{\rm B}T$ is the inverse temperature. The quantum-classical correspondence is derived as

$$\begin{aligned} Z_{\rm Q} &= \sum_{\sigma_0=\pm1}\langle\sigma_0|\Big[\exp\Big(\frac{\beta h_x}{N}\sigma_x\Big)\exp\Big(i\frac{\beta h_z}{N}\sigma_z\Big)\Big]^N|\sigma_0\rangle \\ &= \sum_{\sigma_0}\cdots\sum_{\sigma_{N-1}}\prod_{k=0}^{N-1}\langle\sigma_{k+1}|\exp\Big(\frac{\beta h_x}{N}\sigma_x\Big) \\ &\quad\cdot\exp\Big(i\frac{\beta h_z}{N}\sigma_z\Big)|\sigma_k\rangle \\ &= \sum_{\sigma_0}\cdots\sum_{\sigma_{N-1}}A^N \\ &\quad\cdot\exp\Big[\sum_{k=0}^{N-1}(\beta_{\rm cl}J\sigma_{k+1}\sigma_k + i\beta_{\rm cl}h_{\rm cl}\sigma_k)\Big], \end{aligned} \tag{3}$$

where $\beta_{\rm cl}$ is the effective inverse temperature of the classical system and the parameters of the classical and quantum systems are related to each other by

$$\begin{aligned} &\beta_{\rm cl}J = -\frac{1}{2}\ln\Big[\tanh\Big(\frac{\beta h_x}{N}\Big)\Big],\quad \beta_{\rm cl}h_{\rm cl} = \frac{\beta h_z}{N}, \\ &A = \sqrt{\cosh\Big(\frac{\beta h_x}{N}\Big)\sinh\Big(\frac{\beta h_z}{N}\Big)}. \end{aligned} \tag{4}$$

The right-hand side of Eq. (3) corresponds to the partition function for a classical one-dimensional Ising model. Thus, a non-Hermitian quantum system with inverse temperature β, parameters h_x and h_z can mapped to the 1D Ising spin chain with imaginary magnetic field $h_{\rm cl}\to0$ under the condition of thermodynamic limit $N\to\infty$ and the zero-temperature limit $\beta_{\rm cl}\to\infty$ (see the Supplementary Material, Section S2). In our case, the quantum system described by a parity-time ($\mathcal{PT}$) symmetric non-Hermitian Hamiltonian

$$H_{\mathcal{PT}} = \lambda\begin{pmatrix} ia & 1 \\ 1 & -ia \end{pmatrix}, \tag{5}$$

where λ is an overall coefficient utilized to investigate the Lee–Yang zeros of the 1D Ising model. The corresponding parameters are $h_x = 1$ and $h_z = a$. By adjusting the non-Hermitian parameter a, the systems under different imaginary magnetic fields can be constructed. Eigenvalues of this Hamiltonian are $E_\pm = \pm\lambda\sqrt{1-a^2}$. A pair of exceptional points arise at $a=\pm1$, at which both the eigenvalues and the eigenstates are coalesce. Based on the equivalence of the partition function between the classical Ising model and the non-Hermitian Hamiltonian, we focus on the partition function of $H_{\mathcal{PT}}$:

$$Z_{\mathcal{PT}} \equiv {\rm Tr}[e^{-\beta H_{\mathcal{PT}}}] = \sum_{p\in\{+,-\}}e^{-\beta E_{\rm p}}, \tag{6}$$

The partition function $Z_{\mathcal{PT}}$ takes a real value because the eigenvalues are either real or form a complex conjugate pair due to $\mathcal{PT}$ symmetry. When the eigenvalues are real, corresponding to the $\mathcal{PT}$-symmetric phase, the partition function is always larger than zero. The zeros of partition function can be achieved in the $\mathcal{PT}$-symmetry broken regime, where the imaginary part of eigenvalues appear. The condition for the Lee–Yang zeros is given by $\beta\lambda\sqrt{a^2-1} = (n+1/2)\pi$ for non-negative integer n. These zeros appear at $a = \sqrt{(n+1/2)^2\pi^2/\beta^2\lambda^2+1}$. As β increases, the Lee–Yang zeros are more densely distributed.

In order to obtain the partition function of the non-Hermitian quantum system, i.e., the partition function of the Ising model, the dilation method is implemented to realize the evolution under the non-Hermitian Hamiltonian.[19,20] The evolution under $H_{\mathcal{PT}}$ can be described by the Schrödinger equation $i\partial_t|\psi(t)\rangle = H_{\mathcal{PT}}|\psi(t)\rangle$. The non-unitary evolution of $|\psi(t)\rangle$ can be obtained by introducing an ancilla qubit and projecting the dilated two qubit state, $|\Psi(t)\rangle = |\psi(t)\rangle\otimes|-\rangle + \eta(t)|\psi(t)\rangle\otimes|+\rangle$, into the subspace where the ancilla qubit state is $|-\rangle$. It is noted that $|-\rangle$ and $|+\rangle$ are two eigenstates of the Pauli operator σ_y, which form an orthogonal basis of the ancilla qubit, $\eta(t)$ is an appropriate operator and $|\Psi(t)\rangle$ is unnormalized for convenience. The evolution of state $|\Psi(t)\rangle$ is governed by a Hermitian Hamiltonian $H_{\rm tot}(t)$, which can be flexibly designed according to practical quantum systems (see the Supplementary Material, Section S3). The final state of the coupled system composed of system qubit and ancilla qubit is obtained by quantum state tomography. The system qubit state is achieved by selecting the subspace where the ancilla qubit state is $|-\rangle$ and renormalizing it. By fitting the evolution of final state population with time, the parameter a of the non-Hermitian Hamiltonian can be obtained. From the model of Hamiltonian as shown in Eq. (5), the corresponding eigenvalues, $E_{\rm p}$, can be obtained. The partition function can be obtained from the definition formula (6) with the set inverse temperature β.

A single NV center in diamond is used to construct the non-Hermitian quantum system [Fig. 1(a)]. The Hamiltonian of the NV center can be written as $H_{\rm NV} = 2\pi(DS_z^2 + \omega_e S_z + QI_z^2 + \omega_n I_z + AS_zI_z)$, where $D = 2.87\,{\rm GHz}$ is the zero-field splitting of the electron spin, $Q = -4.95\,{\rm MHz}$ is the nuclear quadrupolar interaction, and $A = -2.16\,{\rm MHz}$ is the hyperfine coupling between the electron spin and the nuclear spin; ω_e (ω_n) denotes the Zeeman splitting of the

electron (nuclear) spin; S_z and I_z are the spin-1 operators of the electron spin and the nuclear spin, respectively. Considering the Hamiltonian of the NV center, we choose

$$H_{\rm tot}(t) = A_1(t)\sigma_x \otimes I + A_2(t) I \otimes \sigma_z + A_3(t)\sigma_y \otimes \sigma_z + A_4(t)\sigma_z \otimes \sigma_z, \quad (7)$$

where $A_i(t)$ represent real value parameters depending on $H_{\mathcal{PT}}$ and the dilation method; σ_x, σ_y and σ_z are Pauli matrices. The operators appearing before and after the direct product symbol in Eq. (7) act on system qubit and ancilla qubit, respectively. The electron spin is chosen as the system qubit and the nuclear spin is selected as the ancilla qubit. The subspace spanned by $|0\rangle_e|1\rangle_n$, $|0\rangle_e|0\rangle_n$, $|-1\rangle_e|1\rangle_n$ and $|-1\rangle_e|0\rangle_n$ [as shown in Fig. 1(a)] is encoded as a two-qubit system to construct $H_{\rm tot}(t)$. An appropriate interaction picture is chosen to transform the diagonal static Hamiltonian of the NV center to the diagonal parts of $H_{\rm tot}(t)$. The off-diagonal parts of $H_{\rm tot}(t)$, which are jumping terms depending on the ancilla qubit states, can be realized by two selective microwave (MW) pulses [blue arrows in Fig. 1(a)] with appropriate amplitudes and phases (see the Supplementary Material, Section S4).

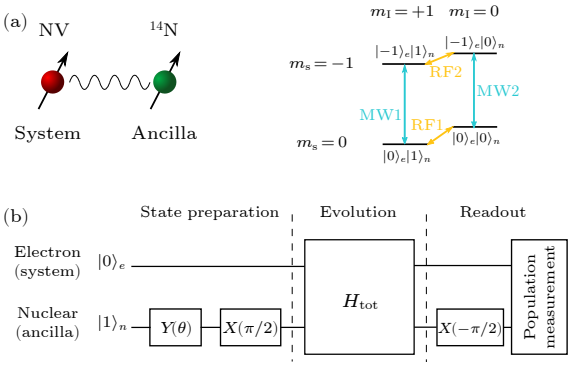

Fig. 1. Construction of non-Hermitian quantum system in NV center. (a) The electron spin is used as the system qubit and the nuclear spin is served as ancilla qubit. The two-qubit system is composed of four energy levels in NV center $|m_S, m_I\rangle = |0, +1\rangle$, $|0, 0\rangle$, $|-1, +1\rangle$, and $|-1, 0\rangle$ labeled by $|0\rangle_e|1\rangle_n$, $|0\rangle_e|0\rangle_n$, $|-1\rangle_e|1\rangle_n$, and $|-1\rangle_e|0\rangle_n$. The electron-spin and nuclear-spin transitions are selectively driven by microwave (MW) pulses (blue arrows) and radio-frequency (RF) pulses (orange arrows), respectively. (b) Quantum circuit of the experiment. X and Y denote the single nuclear spin qubit rotation around the x and y axes. The two-qubit system is prepared to $|\Psi(0)\rangle = |0\rangle_e|-\rangle_n + \eta_0|0\rangle_e|+\rangle_n$ by rotations Y(θ) and $X(\pi/2)$. Then the two-qubit system evolves under the dilation Hamiltonian $H_{\rm tot}(t)$. The populations of the four energy levels are measured after the rotation $X(-\pi/2)$.

The experiments were implemented on an optically detected magnetic resonance setup. The static magnetic field was set to 503 Gauss in order to polarize the NV center to state $|0\rangle_e|1\rangle_n$ by optical pumping.[21] When we choose $\eta(0) = \eta_0 \cdot I$, the initial state of the two-qubit system has the form $|\Psi(0)\rangle = |\psi(0)\rangle \otimes (|-\rangle + \eta_0|+\rangle)$. The initial state $|\psi(0)\rangle$ was set to $|0\rangle_e$. $|\Psi(0)\rangle$ was prepared by the single-qubit rotation $Y(\theta)$ followed by the rotation $X(\pi/2)$ of the nuclear spin [Fig. 1(b)]. The operator $Y(\theta)$ stands for the rotation around y axis with the rotation angle, $\theta = 2\arctan(\eta_0)$. The rotation $X(\pi/2)$ is the single-qubit rotations around x axis to realize transformation between the basis spanned by $\{|0\rangle_n, |1\rangle_n\}$ and the basis spanned by $\{|+\rangle_n, |-\rangle_n\}$ of the nuclear spin qubit. The nuclear spin rotations were realized by radio-frequency (RF) pulses with Rabi frequency calibrated to 20 kHz as shown in Fig. 2(a). Then the system evolved under the dilated Hamiltonian $H_{\rm tot}(t)$ by applying two selective MW pulses. The overall coefficient of $H_{\mathcal{PT}}$ and the total evolution time were set as $\lambda = 150$ kHz and $T = 30$ µs, respectively. To suppress the decoherence during the evolution, an isotopically purified ([^{12}C]=99.999%) diamond was utilized in the experiments. The dephasing time of the electron spin, $T_2^\star$, is measured to be 76 ± 11 µs by utilizing the Ramsey sequence as shown in Fig. 2(b). Finally, the nuclear spin rotation $X(-\pi/2)$, transform the state $|\Psi(t)\rangle = |\psi(t)\rangle_e|-\rangle_n + \eta(t)|\psi(t)\rangle_e|+\rangle_n$ into $|\Phi(t)\rangle = |\psi(t)\rangle_e|1\rangle_n + \eta(t)|\psi(t)\rangle_e|0\rangle_n$ for measurement. The normalization population of the electron spin state $|0\rangle_e|1\rangle_n$ (denoted as P_0) in the subspace of nuclear spin state $|1\rangle_n$ is obtained by $P_0 = P_{|0\rangle_e|1\rangle_n}/(P_{|0\rangle_e|1\rangle_n} + P_{|-1\rangle_e|1\rangle_n})$, with $P_{|0\rangle_e|1\rangle_n}$ ($P_{|-1\rangle_e|1\rangle_n}$) being the population of state $|0\rangle_e|1\rangle_n$ ($|-1\rangle_e|1\rangle_n$).

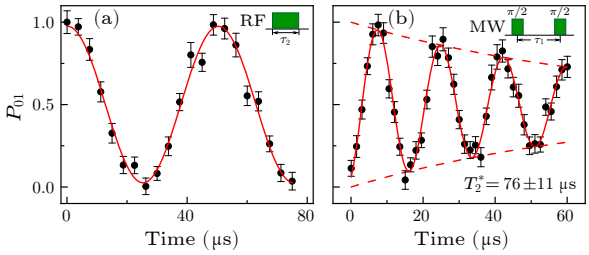

Fig. 2. Rabi frequency of the RF pulses and the coherence time of the electron spin. (a) Result of the Rabi oscillation (insert, pulse sequence) for the nuclear spin. P_{01} is the population of state $|0\rangle_e|1\rangle_n$. The solid red line is fitted to the experimental data (black points). The Rabi frequency is measured to be 19.9 ± 0.3 kHz. (b) Result of the Ramsey experiment (insert, pulse sequence) for the electron spin. The solid red line is fitted to the experimental data (black points), the red dashed line is the fitted to the envelope curve. The decay time is measured to be $T_2^\star = 76 \pm 11$ µs.

Figure 3 shows the evolution under the non-Hermitian Hamiltonian and the measurement of the partition function. The state evolution under $H_{\mathcal{PT}}$ is explored by monitoring P_0. The time of the state evolution is varied from 0 to 30 µs. Figures 3(a)–3(d) show the state evolution under $\mathcal{PT}$ symmetric Hamiltonian with $a = 1.000$ [Fig. 3(a)], $a = 1.040$ [Fig. 3(b)], $a = 1.143$ [Fig. 3(c)] and $a = 1.317$ [Fig. 3(d)]. All errors are one standard deviation with repeating the experiments for 2 million times. The parameter $a_{\rm exp}$ is obtained by curve fitting the experimental time evolution of the population P_0 to theoretical predictions (see the Supplementary Material, Section S5). The fitting results show good agreement with the theoretical predictions as exhibited in Figs. 3(a)–3(d). The eigenvalues of the $H_{\mathcal{PT}}$ can be achieved by $E_\pm^{\rm exp} = \pm\sqrt{1 - a_{\rm exp}^2}$. The partition function at the inverse temperature β can be obtained from Eq. (6). Figures 3(f)

and 3(g) show the measured dependence of the partition function with a at inverse temperature $\beta_1 = 2.837/\lambda$ [Fig. 3(f)] and $\beta_2 = 5.499/\lambda$ [Fig. 3(g)]. For these two inverse temperatures, the first Lee–Yang zeros are located at $a = 1.143$ and $a = 1.040$, respectively, satisfying the condition $\beta\lambda\sqrt{a^2-1} = \pi/2$. As the inverse temperature increases, the first Lee–Yang zero moves towards the critical point $a = 1$, which is shown by the theoretical predictions in Fig. 3(e). At the inverse temperature of $\beta_1 = 2.837/\lambda$, only one zero can be observed in the region of $1.0 < a < 1.4$; while at the higher inverse temperature of $5.499/\lambda$, two zeros can be observed within the same range. This result shows that higher inverse temperature makes the distribution of zeros more dense, consistent with the occurrence of zeros satisfying $\beta\lambda\sqrt{a^2-1} = (n+1/2)\pi$.

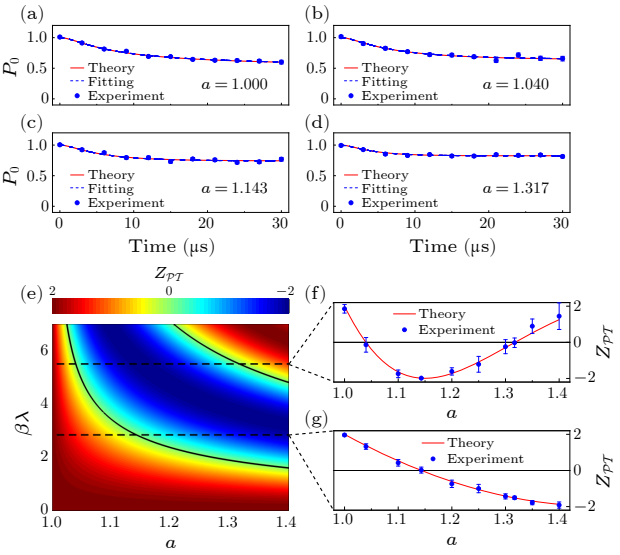

Fig. 3. The partition function obtained from the state evolution under $\mathcal{PT}$ symmetric Hamiltonian. (a)–(d) Experimental state evolution under $\mathcal{PT}$ symmetric Hamiltonians with different parameter a of the Hamiltonian, where $a = 1.000$ (a), $a = 1.040$ (b), $a = 1.143$ (c), and $a = 1.317$ (d). P_0 is the renormalized population of the state $|m_S = 0\rangle$ of the electron spin when the nuclear spin state is in the selected state $|m_I = +1\rangle$. Blue dots are experimental results, blue dashed lines are the fitting results and red lines are the theoretical predictions. (e) The value of the partition function obtained from Eq. (6) with various inverse temperature β. The black solid lines characterize the zeros of partition function. The overall coefficient λ is 150 kHz. [(f), (g)] The partition function of various parameters a at inverse temperature $\beta_1 = 2.837/\lambda$ (f) and $\beta_2 = 5.499/\lambda$ (g).

The partition function fully determines the free energy and the thermodynamic property of the system as $F = -\beta^{-1}\ln Z_{\mathcal{PT}}$. The free energy is an analytic function of the physical parameters, such as temperature and magnetic field, except that it is singular at the Lee–Yang zeros. Here we obtain the free energies for various inverse temperatures from the measured partition function. The results are shown in Fig. 4(a) at the parameter $a = 1.143$. The free energy increases rapidly and tends to infinity as the inverse temperature approaches $\beta_1 = 2.837/\lambda$. At this inverse temperature the partition function $Z_{\mathcal{PT}}$ is zero. In addition, we observe that the errors of the data points increase dramatically as β approaches the Lee–Yang zero in Fig. 4(b). The error is proportional to $\tan(\beta\lambda\sqrt{a^2-1})$. The divergence occurs when β moves towards β_1, while $\beta\lambda\sqrt{a^2-1}$ approaches $\pi/2$. Based on the measured partition function, we successfully reconstruct the asymptotic behavior and singularity of free energy in vicinity of the Lee–Yang zeros.

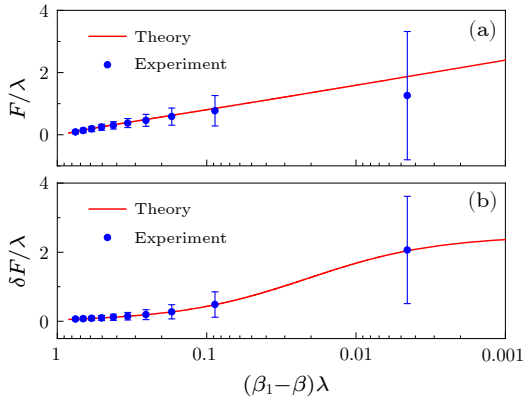

Fig. 4. The free energy reconstructed from the measured partition function. (a) The experimentally determined free energy as the inverse temperature approaches $\beta_1 = 2.837/\lambda$. The overall coefficient λ is 150 kHz. The partition function vanishes at β_1, when the parameter a is set as 1.143. The blue points are the experimental results, and the red line is the theoretical prediction. (b) The error of the free energy with different inverse temperatures. The blue points correspond to the error bars in (a). The red line shows the theoretical expectation that the error is proportional to $\tan(\beta\lambda\sqrt{a^2-1})$. When β approaches β_1, $\beta\lambda\sqrt{a^2-1}$ moves towards $\pi/2$.

Our work build up a non-Hermitian quantum system to investigate the Lee–Yang criticality of the classical one-dimensional Ising model. The Lee–Yang zeros of the one-dimensional Ising model and the critical properties of the free energy near the Lee–Yang zeros are successfully observed. Our work provides the possibility to further use non-Hermitian systems to study the critical problems of the one-dimensional Ising model.[22] For example, the Kibble–Zurek scaling[23] can be investigated by utilizing the time-dependent non-Hermitian Hamiltonian. It should be noted that our method of the equivalent between the partition function of the classical model and the quantum system generally requires a priori information on the partition function of many-body system, so it has only been derived in the case of the one-dimensional Ising model. We also look forward to theoretical breakthroughs that will allow us to study higher-dimensional systems and other universality models through a similar method.

Acknowledgments. This work was supported by the National Key R&D Program of China (Grant No. 2021YFB3202800), the National Natural Science Foundation of China (Grant No. 12174373), the Chinese Academy of Sciences (Grant No. GJJSTD20200001), the Innovation Program for Quantum Science and Technology (Grant No. 2021ZD0302200), and Anhui Ini-

tiative in Quantum Information Technologies (Grant No. AHY050000). X. R. thanks the Youth Innovation Promotion Association of Chinese Academy of Sciences for their support. Yang W. and Ya W. thank the Fundamental Research Funds for the Central Universities for their support. W. L. is funded by Beijing University of Posts and Telecommunications Innovation Group.

References

[1] Chandler D 1987 *Introduction to Modern Statistical Mechanics* (Oxford: Oxford University Press)
[2] Goldenfeld N 1992 *Lectures on Phase Transitions and the Renormalization Group* (Boulder: Westview Press)
[3] Yang C N and Lee T D 1952 *Phys. Rev.* **87** 404
[4] Lee T D and Yang C N 1952 *Phys. Rev.* **87** 410
[5] Lee J 2013 *Phys. Rev. Lett.* **110** 248101
[6] Lee J 2013 *Phys. Rev. E* **88** 022710
[7] Krasnytska M, Berche B, Holovatch Y, and Kenna R 2015 *Europhys. Lett.* **111** 60009
[8] Krasnytska M, Berche B, Holovatch Y, and Kenna R 2016 *J. Phys. A* **49** 135001
[9] Borrmann P, Mülken O, and Harting J 2000 *Phys. Rev. Lett.* **84** 3511
[10] van Dijk W, Lobo C, MacDonald A, and Bhaduri R K 2015 *Can. J. Phys.* **93** 830
[11] Binek C 1998 *Phys. Rev. Lett.* **81** 5644
[12] Binek C, Kleemann W, and Katori H A 2001 *J. Phys.: Condens. Matter* **13** L811
[13] Wei B B and Liu R B 2012 *Phys. Rev. Lett.* **109** 185701
[14] Peng X, Zhou H, Wei B B, Cui J, Du J, and Liu R B 2015 *Phys. Rev. Lett.* **114** 010601
[15] Francis A, Zhu D W, Huerta Alderete C, Johri S, Xiao X, Freericks J K, Monroe C, Linke N M, and Kemper A F 2021 *Sci. Adv.* **7** eabf2447
[16] Suzuki M 1976 *Prog. Theor. Phys.* **56** 1454
[17] Kogut J B 1979 *Rev. Mod. Phys.* **51** 659
[18] Matsumoto N, Nakagawa M, and Ueda M 2022 *Phys. Rev. Res.* **4** 033250
[19] Wu Y, Liu W, Geng J, Song X, Ye X, Duan C K, Rong X, and Du J 2019 *Science* **364** 878
[20] Liu W, Wu Y, Duan C K, Rong X, and Du J 2021 *Phys. Rev. Lett.* **126** 170506
[21] Jacques V, Neumann P, Beck J, Markham M, Twitchen D, Meijer J, Kaiser F, Balasubramanian G, Jelezko F, and Wrachtrup J 2009 *Phys. Rev. Lett.* **102** 057403
[22] Fang S, Zhou Z, and Deng Y 2022 *Chin. Phys. Lett.* **39** 080502
[23] Yin S, Huang G Y, Lo C Y, and Chen P 2017 *Phys. Rev. Lett.* **118** 065701